VI Serbian-Belarusian Symp. on Phys. and Diagn. of Lab. &
Astrophys. Plasma, Belgrade, Serbia, 22 - 25 August 2006
eds. M. Ćuk, M.S. Dimitrijević, J. Purić, N. Milovanović
Publ. Astron. Obs. Belgrade No. 82 (2007), 133-147 *Invited lecture*

SHORT LIVE AFTERGLOW IN PURE NITROGEN AND NITROGEN CONTAINING TRACES OF OXYGEN AND METHANE

F. Krčma, V. Mazánková, I. Soural

Brno University of Technology, Faculty of Chemistry, Purkyňova 118, 612 00 Brno, e-mail: krcma@fch.vutbr.cz

Abstract. The work presents results obtained during spectroscopic observations of DC flowing post-discharges of pure nitrogen plasma and nitrogen plasma containing traces of oxygen and methane. The plasma has been studied by the emission spectroscopy of three nitrogen spectral systems, NO^{β} bands (with oxygen impurities) and two CN spectral systems (when methane was added).

The maximum of the pink afterglow intensity of nitrogen 1^{st} positive system decreased more or less exponentially with increasing the oxygen concentration. The position of the maximal pink afterglow emission was shifted to shorter decay times but both nitrogen positive systems showed a slow increase of the decay time of pink afterglow maximum after the initial shift to the earlier post-discharge position. Intensities of both nitrogen positive systems didn't show any significant dependence on the oxygen concentration. The NO^{β} bands were observed with low intensity and their intensities were directly proportional to the oxygen concentration.

The maxima of the pink afterglow intensities for all three nitrogen systems were decreasing proportionally to the increase of the methane concentration. The position of the maximal pink afterglow emission was also more or less linearly shifted to later decay times, it means on the contrary to the oxygen impurity. The strong CN emission is dominant at methane concentrations beyond 7 ppm and its intensity was more or less directly proportional to the methane concentration in the studied range.

On the basis of the experimental results, the appropriate kinetic models of the plasma generated in pure nitrogen and in nitrogen with oxygen or methane traces were designed. The specific state-to-state energy transfer reactions between the studied states are presented.

1. INTRODUCTION

Nitrogen post-discharges in various configurations have been subjects of many studies for a relatively long time [1-6]. Besides the laboratory and technological plasmas the nitrogen post-discharge is studied also in the kinetics of upper atmosphere (corona borealis [7-9]) and these processes are also taken into account in some extraterrestrial systems, for example in Titan atmosphere [10, 11]. Relaxation processes of atomic and various metastable molecular states created during an active discharge lead to the common thermal equilibrium. Besides collisional processes the light emission plays a significant role in the thermalization. Visible light can be observed up to one second after switching off the active discharge.

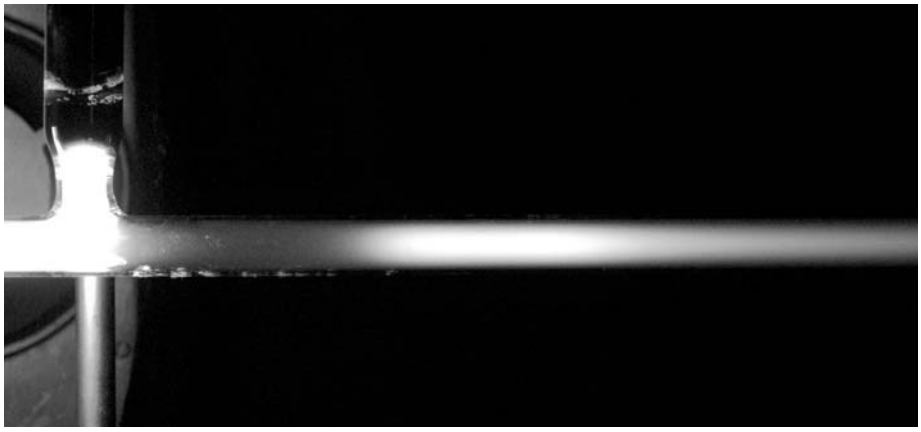

Fig. 1. Pink afterglow in pure nitrogen DC post-discharge.

The first period (up to about 3 ms) of the post-discharge in the pure nitrogen is characterized by a strong decrease of the light emission. After that, the strong light emission at about 5 – 14 ms after the end of an active discharge is known as a pink afterglow (see Fig. 1) and it can be observed in nitrogen only [12, 13]. The pink afterglow is manifested by a strong increase of the pink light emission at the decay times of about 6 – 8 ms in pure nitrogen and of about 28 ms in a nitrogen-argon mixture, while the yellow-orange color is characteristic of the other parts of the nitrogen afterglow. The nitrogen pink afterglow can be characterized as a secondary discharge, because the electron concentration strongly increases due to various collisionally induced ionization processes [14, 15] (see below) and thus the conditions are similar to those in the active discharge. The electron density measurements during the afterglow show the strong increase of the free electron concentration during this post-discharge period [16]. The effect of the nitrogen pink afterglow can be studied only in pure nitrogen; various traces (especially carbon and oxygen) quench it [17]. This work is focused on the experimental study of these

quenching processes. The simplified kinetic model of the post-discharge processes is proposed, too.

2. EXPERIMENTAL SETUP

The DC flowing post-discharge was used for the experimental study. The simplified schematic drawing of the experimental set up is given in Fig. 2.

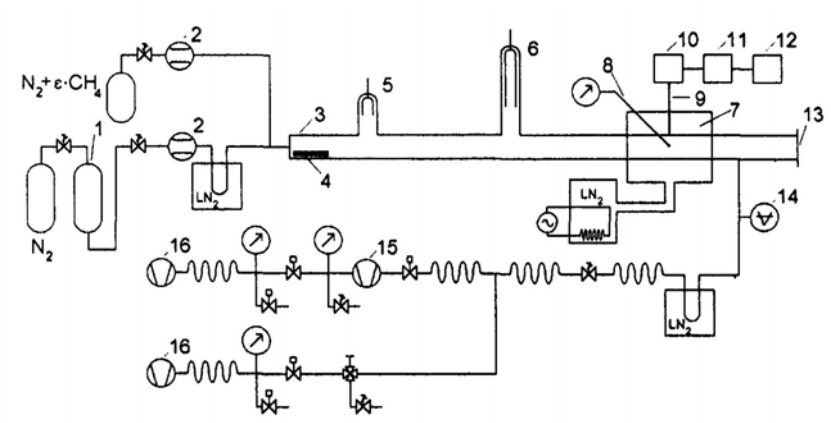

Fig. 2. Siplified scheme of the experimental set-up [17].

An active discharge was created in a Pyrex discharge tube (length: 1100 mm, inner diameter: 16 mm) with a 120 mm electrode distance. Tantalum or molybdenum electrodes were placed in the side arms of the main discharge tube for minimizing the sputtering of the electrode material and also for suppressing the light emitted in the electrode regions. The gas flow was automatically controlled by mass flow controllers. The nitrogen was of 99.999 % purity and it was further cleaned by copper based catalyzer and liquid nitrogen trap. The synthetic air (80 % N_2 + 20 % O_2) and various nitrogen-methane mixtures (except commercial mixture of 1 % of methane in pure nitrogen) were prepared directly in the laboratory and their compositions were measured by the gas chromatography. The system was pumped continuously by a rotary oil pump. The total pressure in the discharge tube during the experimental studies was measured by a baratron and Pirani gauges connected to the end of the discharge tube.

The spectra emitted from the post-discharge were measured by Jobin Yvon monochromator (HR320 or TRIAX 550 with the 1200 grooves per mm grating) coupled with multichannel detectors. The emitted light was led to the entrance slit of the monochromator by the multimode quartz optical fiber movable along the discharge tube. Nitrogen 1st (N_2 ($B\ ^3\Pi_g$) $\rightarrow$ ($A\ ^3\Sigma_u^+$)) and 2nd (N_2 ($C\ ^3\Pi_u$) $\rightarrow$ ($B\ ^3\Pi_g$)) positive and nitrogen 1st negative (N_2^+ ($B\ ^2\Sigma_u^+$) $\rightarrow$ ($X\ ^2\Sigma_g^+$)) systems were recorded

in all spectra. The bands of NO^{β} system ($NO\,(B\,^2\Pi) \rightarrow NO\,(X\,^2\Sigma^+)$) were remarkable with low emission intensity when oxygen was added, CN red ($CN\,(A\,^2\Pi) \rightarrow (X\,^2\Sigma^+)$) and violet ($CN\,(B\,^2\Sigma^+) \rightarrow (X\,^2\Sigma^+)$) systems were observed with higher intensities when methane traces were added. The typical experiment was carried out at total gas pressure of 1000 Pa and discharge current of 150 – 200 mA.

3. QUENCHING BY OXYGEN TRACES

The post-discharge emission intensity profiles of representative bands of all three observed nitrogen spectral systems are shown in Figs. 3 – 5 as a function of the oxygen concentration. The pink afterglow is quenched by oxygen traces. This effect differs for each of the measured nitrogen systems as it is compared in Fig. 6 where the dependences of the pink afterglow maximal intensities on the oxygen concentration are given. At the lower concentrations (up to about 200 ppm), the significant increase of the nitrogen positive band intensity can be seen.

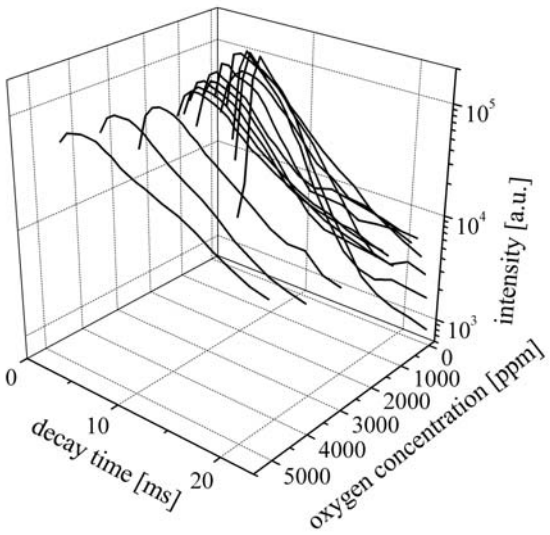

Fig. 3. Intensity of nitrogen 1st positive 2–0 band during the pink afterglow as a function of oxygen concentration.

The slow decrease of emission intensity with the increasing oxygen concentration appeares at higher concentrations but at the highest concentrations, another slight increase can be recognised. The emission from molecular ion decreases more or less exponentially with oxygen concentration increasing in the whole concentration range.

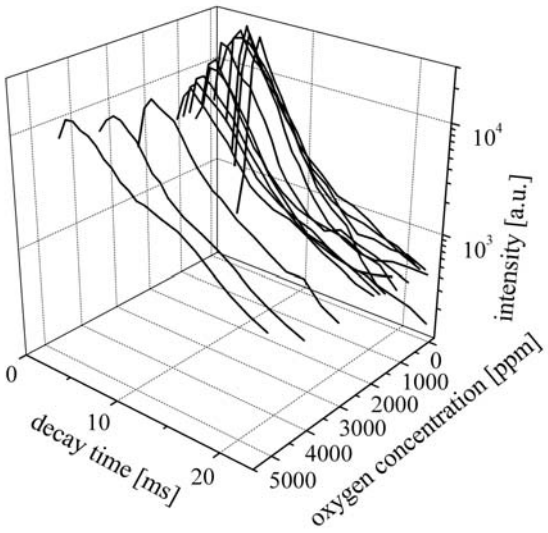

Fig. 4. Intensity of nitrogen 2nd positive 0–0 band during the pink afterglow as a function of oxygen concentration.

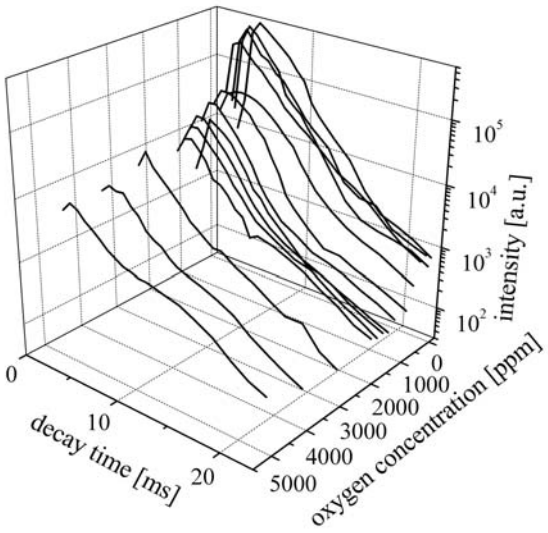

Fig. 5. Intensity of nitrogen 1st negative 0–0 band during the pink afterglow as a function of oxygen concentration.

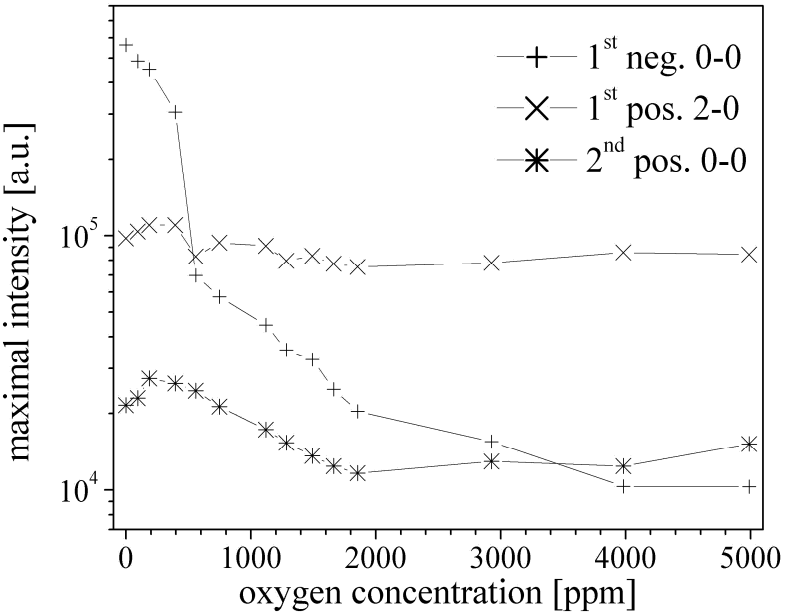

Fig 6. Maximal pink afterglow emission intensity as a function of oxygen concentration.

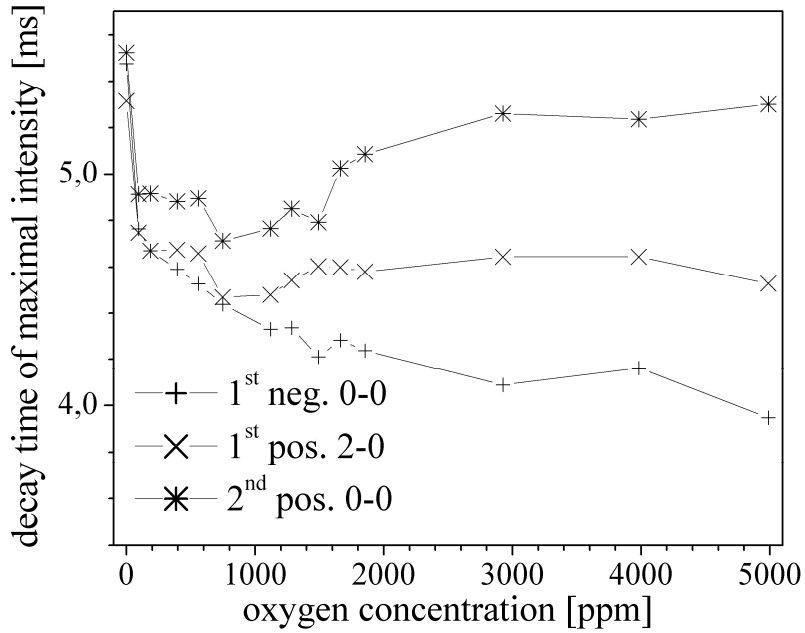

Fig. 7. Position of the maximal pink afterglow emission intensity as a function of oxygen concentration.

The position of the maximal pink afterglow emission intensity depends on oxygen concentration, too, as it is demonstrated in Fig. 7. The positions of maxima were calculated using the fitting of the post-discharge profile by polynomial function of 3rd order in time interval of 3 – 8 ms due to the limited number of experimental points (we didn't expect the observed effect and thus the number of experimental points was not sufficient to use the original time scale). The maximum of the 1st negative system is shifted to earlier post-discharge positions at the lower oxygen concentration (under about 100 ppm), but further increase of oxygen amount has only a slight influence of the same character. Both nitrogen positive systems show a slow increase of the decay time of pink afterglow maximum after the initial shift to the earlier post-discharge position.

4. QUENCHING BY METHANE TRACES

The pink afterglow quenching by methane traces is about two orders stronger than quenching by oxygen. Experiments focused on quenching by methane were carried out using the discharge tube with higher diameter. Due to the fact that the wall processes play a significant role in the post-discharge kinetics the pink afterglow maximum in pure nitrogen is localised at longer decay time of 8 ms in this case.

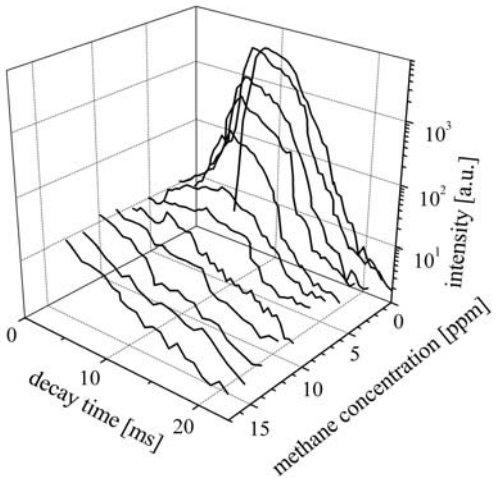

Fig. 8. Intensity of nitrogen 2nd positive 0–2 band during the pink afterglow as a function of methane concentration.

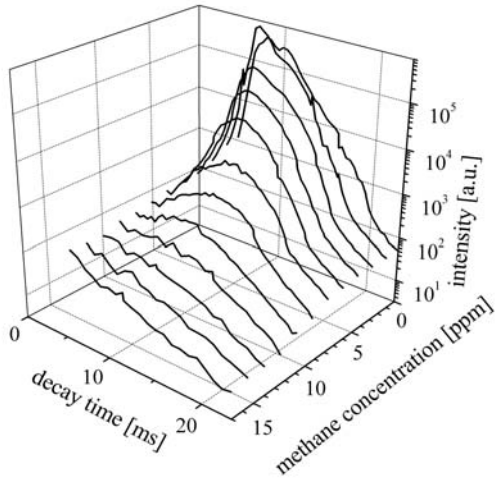

Fig. 9. Intensity of nitrogen 1st negative 0–0 band during the pink afterglow as a function of methane concentration.

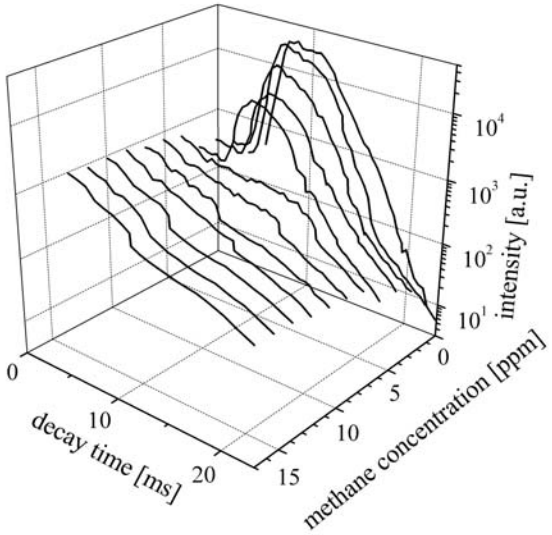

Fig. 10. Intensity of nitrogen 1st negative 1–1 band overlaped by P-branch of CN violet 0-0 band during the pink afterglow as a function of methane concentration.

The influence of methane presence on the pink afterglow has been observed through the emission of the nitrogen 1st negative and 2nd positive and CN violet spectral systems. The other spectral systems (nitrogen 1st positive and CN red) have been observed only in the other experiments and they show similar behaviours. Figures 8 – 10 show measured band head intensities of selected bands as a function of the methane concentration during the pink afterglow. The intensity profiles of the 1st negative 0–0 and 2nd positive 0–2 bands are similar, the second one is less

obvious due to lower intensities. Different situation is in the case of 1st negative 1–1 band which is completely overlapped by the P branch of 0–0 CN violet spectral system (see Figure 10). Thus at methane concentrations up to 7 ppm, the effect of the pink afterglow can be resolved, at higher concentrations, the strong CN emission can be dominant and its intensity is more or less directly proportional to the methane concentration in the studied range (in Fig. 10 it looks like independent due to the overlap by exponentially quenched nitrogen 1st negative band).

Figures 11 and 12 show the quenching of maximal pink afterglow intensity by methane addition and shift of this maximal intensity in the post-discharge time. Fig. 11 shows the dependence of the pink afterglow maximal intensity on the methane concentration. A small increase of the intensity can be seen at methane concentrations up to about 1 ppm and after that the maximum intensity is exponentially quenched by methane. At concentrations higher than 12 ppm, the maximum of the pink afterglow can't be found, however, this effect still exists. Fig. 12 demonstrates the shift of the pink afterglow intensity maximum to later decay times. This effect is more or less directly proportional to the methane concentration. The maximum pink intensity shifts up to 15.5 ms at the highest methane concentration of about 12 ppm when the effect can be measured. The shift of pink afterglow maximal intensity by methane on contrary to the shift by oxygen addition.

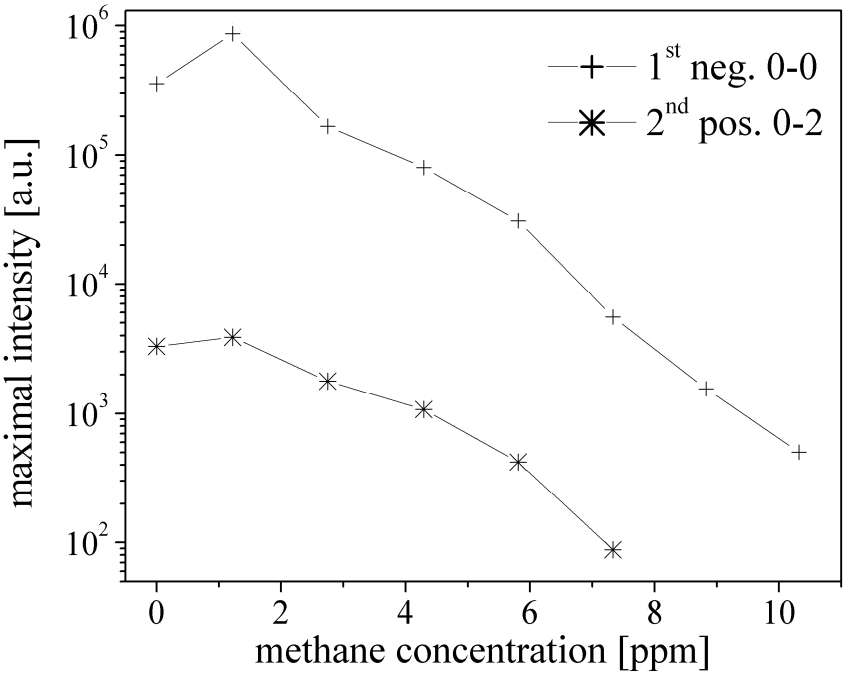

Fig. 11. Maximal pink afterglow emission intensity as a function of methane concentration.

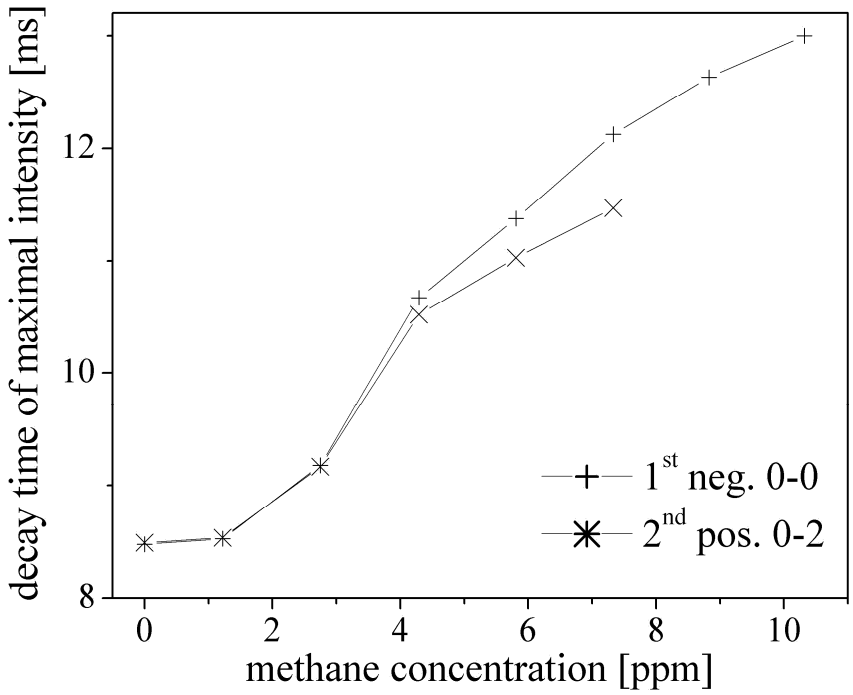

Fig. 12. Position of the maximal pink afterglow emission intensity as a function of methane concentration.

5. KINETIC MODEL

The nitrogen afterglow kinetics is a really complicated problem. The mechanisms that populate the radiative states of a neutral molecule and a molecular ion are different and they must be discussed separately. After that, the kinetics in both nitrogen mixtures is discussed. Only the creation mechanisms are given in the schemes. Besides them, many collisional quenching processes of specific states must be included to the numeric modeling (see [18]).

5.1 Neutral nitrogen

The $N_2(B\,^3\Pi_g)$ and $N_2(C\,^3\Pi_u)$ states are dominantly created by pooling reactions of lower metastable states, especially by the vibrational excited ground state and by the lowest 8 levels of $N_2(A\,^3\Sigma_u^+)$ state [2-4, 19]. These reactions show the creation of both these states, but they cannot explain the strong population enhancement during the pink afterglow. Therefore another process must be considered. It is known that in nitrogen post-discharge kinetics of the ground state

the initial vibrational distribution changes by v-v process into the Treanor-Gordiets distribution that can be characterized by the significant enhancement of populations at higher vibrational levels. In the creation of the $N_2(B\ ^3\Pi_g)$ and $N_2(C\ ^3\Pi_u)$ states by pooling, the ground state must be excited at least to the levels of $v = 4$, or $v = 19$ respectively, when the pooling is with $N_2(A\ ^3\Sigma_u^+)$ state. When two ground states are involved the excitation to the $v = 14$, or $v = 24$ respecitively, is necessary. It is clear that at the end of an active discharge all these species are presented in the gas but their concentrations are much lower than the concentrations of the lowly excited molecules. The creation of higher vibrational levels takes some time, of course, and thus the dark space between the end of the active discharge and the pink afterglow can be observed. The pooling reactions can also lead to the creation of the $N_2(A\ ^3\Sigma_u^+)$ state, and thus the pink afterglow effect is further enhanced. The reaction scheme can be written as follows (for references and rate constants see [20]):

$$N_2(X\ ^1\Sigma_g^+, v) + N_2(X\ ^1\Sigma_g^+, w) \rightarrow N_2(X\ ^1\Sigma_g^+, v+1) + N_2(X\ ^1\Sigma_g^+, w-1) \quad \text{R1}$$

$$2\ N_2(X\ ^1\Sigma_g^+, v \geq 12) \rightarrow N_2(A\ ^3\Sigma_u^+) + N_2 \quad \text{R2}$$

$$N_2(X\ ^1\Sigma_g^+, v \geq 25) + N(^4S_0) \rightarrow N_2(A\ ^3\Sigma_u^+) + N(^4S_0) \quad \text{R3}$$

$$N_2(X\ ^1\Sigma_g^+, v \geq 25) + e \rightarrow N_2(A\ ^3\Sigma_u^+) + e \quad \text{R4}$$

$$N_2(X\ ^1\Sigma_g^+, v \geq 35) + N(^4S_0) \rightarrow (N_2(a\ ^1\Pi_g) \text{ or } N_2(a'\ ^1\Sigma_u^-)) + N(^4S_0) \quad \text{R5}$$

$$N_2(X\ ^1\Sigma_g^+, v \geq 35) + e \rightarrow (N_2(a\ ^1\Pi_g) \text{ or } N_2(a'\ ^1\Sigma_u^-)) + e \quad \text{R6}$$

$$2\ N_2(X\ ^1\Sigma_g^+, v \geq 14) \rightarrow N_2(B\ ^3\Pi_g) + N_2 \quad \text{R7}$$

$$N_2(X\ ^1\Sigma_g^+, v \geq 4) + N_2(A\ ^3\Sigma_u^+) \rightarrow N_2(B\ ^3\Pi_g) + N_2 \quad \text{R8}$$

$$2\ N_2(A\ ^3\Sigma_u^+) \rightarrow N_2(B\ ^3\Pi_g) + N_2 \quad \text{R9}$$

$$2\ N_2(X\ ^1\Sigma_g^+, v \geq 24) \rightarrow N_2(C\ ^3\Pi_u) + N_2(X\ ^1\Sigma_g^+) \quad \text{R10}$$

$$N_2(X\ ^1\Sigma_g^+, v \geq 19) + N_2(A\ ^3\Sigma_u^+) \rightarrow N_2(C\ ^3\Pi_u) + N_2 \quad \text{R11}$$

$$2\ N_2(A\ ^3\Sigma_u^+) \rightarrow N_2(C\ ^3\Pi_u) + N_2(X\ ^1\Sigma_g^+) \quad \text{R12}$$

$$N_2(A\ ^3\Sigma_u^+) + N_2(B\ ^3\Pi_g) \rightarrow N_2(C\ ^3\Pi_u) + N_2(X\ ^1\Sigma_g^+) \quad \text{R13}$$

The first six reactions form the precursors, the other lead to the formation of both radiative states. The reaction R1 is well known as v-v pumping process and plays the significant role during the whole nitrogen afterglow. Also the reaction R2 is running about all the time without any significant changes. The reactions R3 – R6 are probably the most important for the pink afterglow creation. They need highly vibrationally excited ground state molecules that are not presented during the afterglow beginning in higher concentrations and they must be created by *v-v* process (reaction R1). This takes some time and after that the electronically excited molecules are created and consequently they can react with molecules excited to the lower vibrational levels. This mechanism can explain the lower radiative afterglow part between the active discharge and the pink afterglow. The other metastable states, especially metastable singlet states, must be, of course, included in the scheme, when a numeric modeling would be used. This simplified reaction scheme clearly demonstrates the main principles of the pink afterglow creation. Much more complex description of the mechanisms was described recently in [12, 21].

5.2 Nitrogen molecular ion

The kinetics of the molecular ion radiative state is more complicated and it can be explained in a two-step scheme. Before the pink afterglow the charged particles concentration is very low [16] but during the pink afterglow it significantly increases. So, the first step must lead to the molecular ion creation.

Due to the fact that the post-discharge is without any external energy source, some of the kinetic processes must be efficient enough for the ionization. The whole process is known as a step-wise ionization [14, 15]. In its principle, the highly excited neutral metastable molecules (excited both electronically and vibrationally) can have energy sufficient for the ionization during their collisions. Precursors for the ionizing collisions are created by the process R1 and by processes similar to R2.

When the molecular ion is created, the excitation to the radiative state must be completed. Recent studies have demonstrated that the main process responsible for the population of the radiative $N_2^+(B\ ^2\Sigma_u^+)$ state is the collisionally induced energy transfer from the vibrationally excited neutral ground state [19] as it is shown as the reaction R18.

The reactions describing kinetics of the molecular ion are, besides the reaction R1, as follows:

$$N_2(X\ ^1\Sigma_g^+, v) + N_2(X\ ^1\Sigma_g^+, w) \rightarrow N_2^* + N_2 \quad \text{R14}$$
$$2\ N_2(X\ ^1\Sigma_g^+, v \geq 32) \rightarrow N_2^+(B\ ^2\Sigma_u^+) + N_2 + e \quad \text{R15}$$
$$N_2(X\ ^1\Sigma_g^+, v) + N_2^* \rightarrow N_2^+ + N_2 + e \quad \text{R16}$$
$$2\ N_2^* \rightarrow N_2^+ + N_2 + e \quad \text{R17}$$
$$N_2(X\ ^1\Sigma_g^+, v \geq 12) + N_2^+(X\ ^2\Sigma_g^+) \rightarrow N_2(X\ ^1\Sigma_g^+) + N_2^+(B\ ^2\Sigma_u^+) \quad \text{R18}$$

The N_2^* in the reactions above means an electronically excited metastable neutral molecule, especially $N_2(A\ ^3\Sigma_u^+)$, $N_2(a\ ^1\Pi_g)$ and $N_2(a'\ ^1\Sigma_u^-)$ states.

5.3 Nitrogen with oxygen traces

Kinetics of pure nitrogen with a small addition of oxygen can be generally described by following additional reactions. The reactions with molecular oxygen can be neglected because we can assume high molecular oxygen dissociation in an active discharge (residence time about 8 ms) and recombination forming molecular oxygen during afterglow can be neglected due to its low concentration.

$$N_2(X\ ^1\Sigma_g^+, v \geq 13) + O \rightarrow NO(X\ ^2\Pi) + N(^4S_0) \quad \text{R19}$$
$$N_2(A\ ^3\Sigma_u^+) + O \rightarrow NO(X\ ^2\Pi) + N(^2D_0) \quad \text{R20}$$
$$N(^4S_0) + O + N_2 \rightarrow NO(X\ ^2\Pi) + N_2 \quad \text{R21}$$
$$NO(X\ ^2\Pi) + N(^4S_0) \rightarrow N_2(X\ ^1\Sigma_g^+, v \cong 3) + O \quad \text{R22}$$
$$N_2(A\ ^3\Sigma_u^+) + NO(X\ ^2\Pi) \rightarrow N_2(X\ ^1\Sigma_g^+, v = 0) + NO(A\ ^2\Sigma^+) \quad \text{R23}$$
$$N_2(X\ ^1\Sigma_g^+, v \geq 23) + NO(X\ ^2\Pi) \rightarrow N_2(X\ ^1\Sigma_g^+) + NO(A\ ^2\Sigma^+) \quad \text{R24}$$

$$N\,(^4S_0) + O + N_2 \rightarrow NO\,(B\,^2\Pi,\ v = 0) + N_2 \qquad R25$$

These reactions show four different channels of NO molecule formation. The reaction R19 has a strong influence on the *v*-*v* process described by reaction R1. Thus highly excited molecular states are formed with lower probability and the creation of electronically excited states is decreased. Formation of nitrogen molecular ion strongly decreases also due to reactions R20, R23 and R24, and thus the nitrogen 1st negative system is effectively quenched. High vibrationally excited ground state nitrogen molecules (over $v = 22$) play a minor role in the formation of electronically excited states, and thus both nitrogen positive systems are quenched only slightly. Direct confirmation of processes described by reaction R23 and R24 is impossible in our contemporary experimental set up because the NO^{γ} system emission is in UV region under 300 nm and a strong light absorption of the Pyrex reactor walls takes part.

5.4 Nitrogen with methane traces

Situation in nitrogen with methane traces is more or less similar as in the previous case. Again we can suppose high dissociation of methane during the active discharge and CN and NH radicals are formed. The NH radicals have not been identified in the spectra, so we suppose that their role in post-discharge kinetics is negligible. The CN radical kinetics can be described in a simplified form by the following scheme:

$$N\,(^4S_0) + C\,(^3P) + M \rightarrow CN + M \qquad R26$$

$$N_2^{*} + CN \rightarrow N_2 + N + C \qquad R27$$

$$N_2\,(X\,^1\Sigma_g^+,\ v \geq 4) + CN\,(X\,^2\Sigma) \rightarrow N_2\,(X\,^1\Sigma_g^+) + CN\,(A\,^2\Pi) \qquad R28$$

$$N_2\,(X\,^1\Sigma_g^+,\ v \geq 12) + CN\,(X\,^2\Sigma) \rightarrow N_2\,(X\,^1\Sigma_g^+) + CN\,(B\,^2\Sigma^+) \qquad R29$$

Reaction R26 represents the CN radical formation by three body recombination (M means a third body, in our case it is mainly nitrogen neutral molecule or the reactor wall). The other two processes are nearly resonant [19, 22] and due to the high concentration of the vibrationally excited neutral nitrogen ground states, they are very effective sources for the strong CN spectra emission.

The reactions R28 and R29 play a significant role in the *v*-*v* process described by the reaction R1. Due to the fact that the excited states of the CN radical are radiative, the reactions R28 and R29 can be repeated many times, and thus the *v*-*v* process could not effectively populate the higher vibrational level needed for the creation of all higher states. Moreover, the reaction R27 effectively decreases the concentration of the electronically excited nitrogen states. Thus the $N_2\,(B\,^3\Pi_g)$, $N_2\,(C\,^3\Pi_u)$ and N_2^+ species could not be formed as effectively as in pure nitrogen, and therefore the pink afterglow is quenched. The strong quenching of nitrogen 1st negative system is caused by the strong depopulation of $N_2\,(X\,^1\Sigma_g^+,\ v \geq 12)$ by reaction R29 that is faster process than reaction R12. Due to this fact, the pink afterglow quenching by methane traces is much more stronger than quenching by

oxygen traces where is no direct reaction depopulating vibrational level of N_2 ($X\ ^1\Sigma_g^+$, $v = 12$).

6. CONCLUSION

The work presents results obtained during spectroscopic observations of DC flowing post-discharges of pure nitrogen plasma and nitrogen plasma containing traces of oxygen and methane. The plasma has been studied by the emission spectroscopy of three nitrogen spectral systems, NO^{β} bands (with oxygen impurities) and two CN spectral systems (when methane was added).

First, the quenching of the nitrogen pink afterglow by the oxygen traces was studied. It was shown that the maximum of the pink afterglow intensity of nitrogen 1st positive system decreased more or less exponentially with the increasing oxygen concentration. The position of the maximal pink afterglow emission was shifted to shorter decay times at the lower oxygen concentration (under about 100 ppm), but further increase of oxygen amount had only a slight influence of the same character. Both nitrogen positive systems showed a slow increase of the decay time of pink afterglow maximum after the initial shift to the earlier post-discharge position. Intensities of both nitrogen positive systems didn't show any significant dependence on the oxygen concentration. The NO^{β} bands were observed with low intensity and their intensities were directly proportional to the oxygen concentration.
The quenching of the nitrogen pink afterglow by the methane traces showed different character of behaviors. It was shown that the maxima of the pink afterglow intensities for all three nitrogen systems were decreasing proportionally to the increase of the methane concentration. The position of the maximal pink afterglow emission was also more or less linearly shifted to later decay times, it means on the contrary to the oxygen impurity. The strong CN emission is be dominant at methane concentrations over about 7 ppm and its intensity was more or less directly proportional to the methane concentration in the studied range.
On the basis of the experimental results, the appropriate kinetic models of the plasma generated in pure nitrogen and in nitrogen with oxygen or methane traces were designed. The specific state-to-state energy transfer reactions between the studied states were presented. The full kinetic models of nitrogen-oxygen and nitrogen-methane mixtures are contemporary under preparation.

This work was supported by the Czech Science Foundation, contracts No. 202/98/P258 and 202/05/0111.

REFERENCES

1. G. E. Beale, H. P. Broida: J. Chem. Phys. **31**, 1030 (1959).
2. L. G. Piper: J. Chem. Phys. **88**, 231 (1988).
3. L. G. Piper: J. Chem. Phys. **88**, 6911 (1988).
4. L. G. Piper: J. Chem. Phys. **91**, 864 (1989).

5. V. Guerra, P. A. Sa, J. Loureiro: J. Phys. D, Appl. Phys. **34** (2001) 1745.
6. F. Krčma: Acta Phys. Slovaka **55**, 453 (2005).
7. Ø. Lie-Svendsen, M. H. Rees, K. Stamnes, E. C. Whipple: Planet. Space Sci. **39**, 929 (1991).
8. A. S. Kirillov, G. A. Aladjev: Adv. Space Res. **16**, 105 (1995).
9. J. S. Morrill, W. M. Benesch: J. Geophys. Res. Space Phys. **101** (1996).
10. C. N. Keller, V. G. Anicich, T. E. Cravens: Planet. Space Sci. **46,** 1157 (1998).
11. V. Dimitrov, A. Bar-Nun: Prog. Reac. Kin. Mechanisms **29**, 1 (2004).
12. P. A. Sa, V. Guerra, J. Loureiro, N. Sadeghi: J. Phys. D, Appl. Phys. **37**, 221 (2004).
13. Loureiro J, Sa PA, Guerra V: J. Phys. D, Appl. Phys. **39**, 122 (2006).
14. L. S. Polak, D. I. Sloveckii, A. S. Sokolov: Opt. Spectrosc. **32**, 247 (1972).
15. F. Paniccia, C. Gorse, M. Cacciatore, M. Capitelli: J. Appl. Phys. **61**, 3123 (1987).
16. J. Janča, A. Tálský, N. El Kattan: Folia Physica **27**, 23 (1978).
17. F. Krčma, L. Babák: Czech. J. Phys. **49**, 271 (1999).
18. C. D. Pintassilgo, J. Loureiro, V. Guerra: J. Phys. D, Appl. Phys. **38**, 417 (2005).
19. F. Krčma, E. T. Protasevich: Post-discharges in Pure Nitrogen and in Nitrogen Containing Halogenated Hydrocarbon Traces, Tomsk Polytechnic University Publishing, Tomsk 2003.
20. F. Krčma: http://www.fch.vutbr.cz/home/krcma/publications/95-thesis-appendix1.pdf.
21. N. Sadeghi, C. Foissac, P. Supiot: J. Phys. D, Appl. Phys. **34,** 1779 (2001).
22. J. Hubeňák, F. Krčma: J. Phys. D, Appl. Phys. **33,** 3121 (2000).